JOURNAL OF THE CANADIAN SOCIETY OF EXPLORATION GEOPHYSICISTS
VOL. 21, NO. 1 (DEC. 1985), P. 7-14

SHALLOW SUB-BOTTOM IMPEDANCE STRUCTURES USING AN ITERATIVE ALGORITHM AND EMPIRICAL CONSTRAINTS

D. CASE CAULFIELD[2], DAVID D. CAULFIELD[1] AND YUNG-CHANG YIM[1]

ABSTRACT

The paper deals with the use of a new iterative algorithm to find the impedance structure of sub-bottom sediments. The system uses normal incident marine seismic data, and empirical relationships between density and porosity and porosity and impedance originally developed by Hamilton and Bachman. The essential idea of the system is that the standard theoretical absorption correction, derived from an exponential dependency, is only a first approximation. Empirical absorption data supplied by Hamilton are substituted and used iteratively to correct the reflected energies until the porosity values from Bachman's curve are stabilized. The paper also examines the iterative algorithm that calculates the reflection coefficients. The system promises to be a quick and accurate way of delineating soil type and sub-bottom structure. Applications include dredging material estimates, rig site surveys, and pipeline route locations where extensive core data are needed. The technique allows for a reduction in the number of cores required, and/or improved material identification for core-to-core correlation. Samples of input data and processing details are supplied, as well as a discussion of final results.

INTRODUCTION

The desire to classify marine surface and sub-bottom sediments from normal incidence data has been a goal of many researchers for a number of years. Hamilton *et al.* (1970), Hamilton and Bachman (1982), Breslau (1964) and Caulfield *et al.* (1976, 1982) have attempted over the past twenty years to relate acoustic impedance measurements to sediment type. The work of Hamilton in the mid 70s provided the first model for the extension of the surface reflection data to the sub-bottom (Caulfield *et al.*, 1982).

This model approximated the absorption loss by an exponential function proportional to frequency and material type. It used various algorithms to correct for the nonlinear parameters of source, and geometry to estimate total apparent plane wave energy incident on the bottom.

This process is known as the Acoustic Core System and has had limited success as a backup to normal shallow-marine survey procedures and core analysis. As more core data have become available, with better lithologic descriptions (detailed descriptions of density, porosity and grain size as a function of depth), the limitations of the model have been defined. Specifically, significant improvement can be made by using a revised reflectivity method and realistic absorption models.

The prediction of actual soil types has been abandoned in favour of the prediction of acoustic properties. This leaves the definition of the lithology of each site to the local geotechnical engineer or geophysicist.

DATA ACQUISITION

Shallow sub-bottom data are normally acquired with a sound source (Boomer, Sparker, Geopulse) and a towed array spatially optimized for the frequencies employed. Because of the relatively high frequencies used (500 Hz - 5 KHz), absorption is more critical than in standard marine seismic operations.

The data are normally recorded in analog form, since the high frequencies employed would create an unmanageable data set with present digital recording techniques. New optical disks might present an economic way for recording the data in a digital format. The choice of sound source and receiver array is dependent on the resolution and depth of penetration required.

METHODS

The present algorithm for predicting acoustic impedance as a function of depth uses single-channel normal incident reflectivity data acquired with the sound sources listed above. Figure 1 shows a typical field record generated by using a new colour display, in which colour is a function of amplitude. This method expands the visual dynamic range from 15-20 dB to 45-50 dB.

Figure 2 illustrates the processing procedures for the present reflection and impedance algorithm. Each step is briefly described as:

1. Analog-Digital Conversion: Rates of 5 to 10 times the Nyquist frequency to preserve phase and absorption data.

[1]Caulfield Engineering, Nisku, Alberta
[2]Dome Petroleum, Calgary, Alberta, formerly of Caulfield Engineering

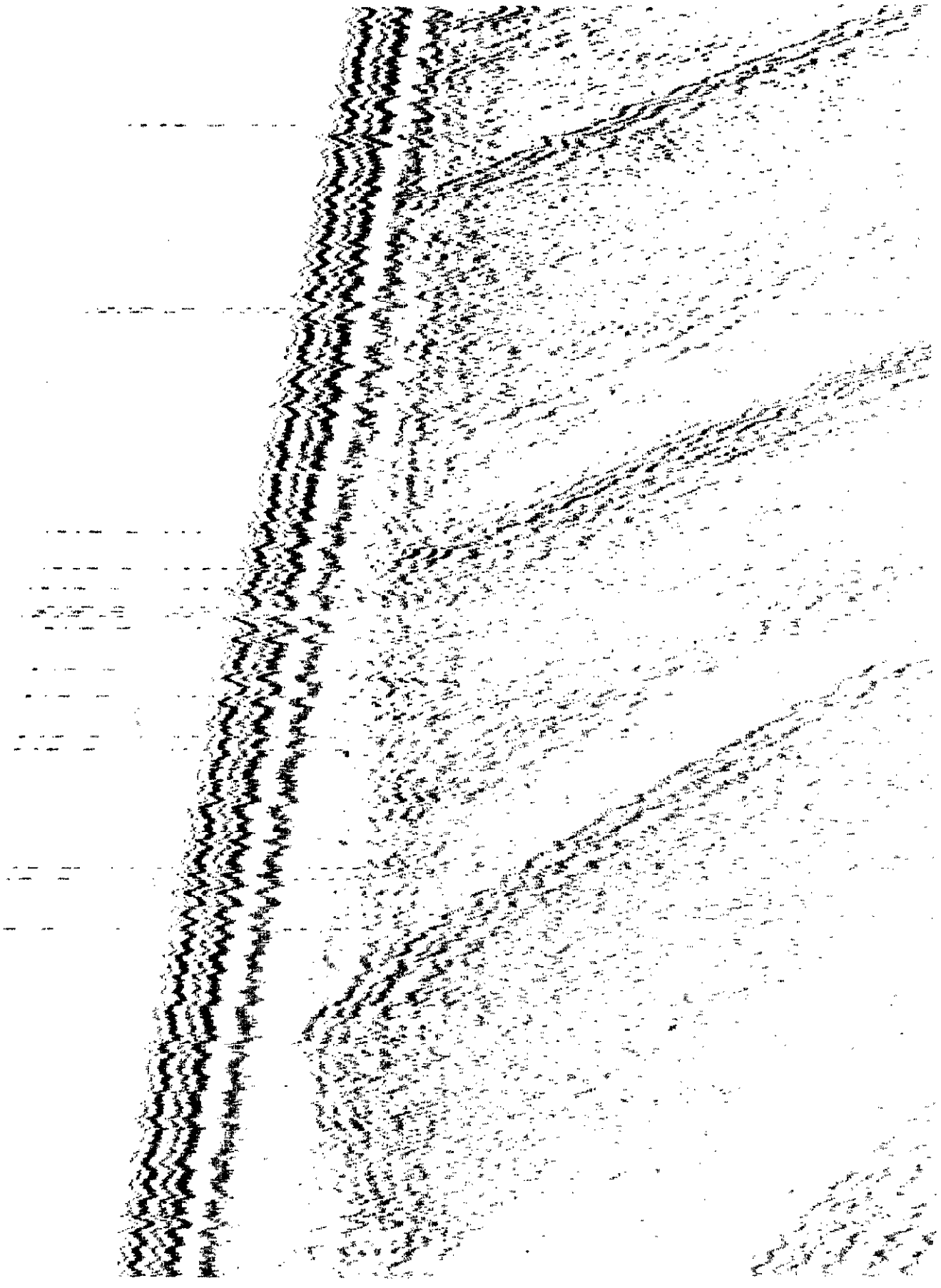

Fig. 1. Typical field record.

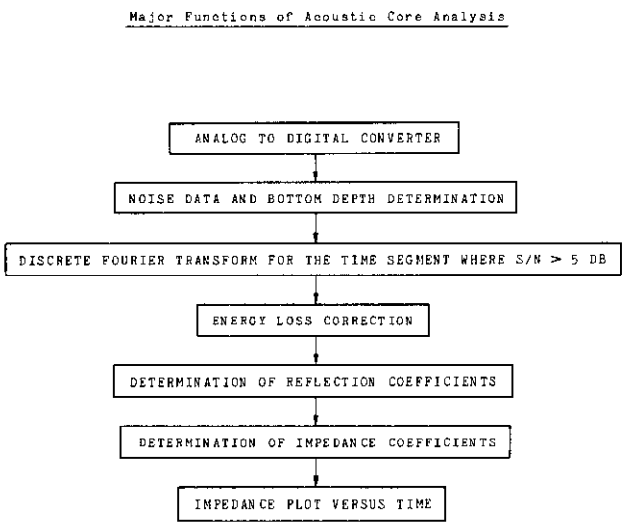

Fig. 2. Major functions of acoustic core analysis.

2. Noise and Plane Wave Corrections: Energy level of the noise is determined from a sample of the ambient noise prior to the bottom return. The energy level of this noise sample is then subtracted from the energy of each layer. Spherical spreading corrections are made by means of standard plane wave transformations.
3. Discrete Fourier Transformation: This process is used to obtain the energy spectrum for each layer.
4. Energy Loss Correction: This provides a correction for the layer loss due to absorption by assuming a simple exponential absorption correction (Hamilton's initial data) as a function of frequency.

   The formula for this correction is:

$$E_i = E_n e^{(\rho\omega/CB)X_n} \tag{1}$$

   where E_i = the corrected energy for the layer i
   E_n = the original layer energy minus the noise
   ρ = layer density
   ω = angular frequency
   B = dimensional constant proportional to viscosity
   C = sound velocity
   X_n = current layer depth from water bottom interface

   The total energy (E_o) incident then is simply equal to the summation of the E_i (layer energies).

$$E_o = K \sum_{i=1}^{N} E_i \tag{2}$$

   where N = number of layers
   K = constant to be identified later

   Obviously, if the system employed can measure radiated sound levels and spectra directly, then this step is not an approximation. Some field systems now allow this, though normally costs have been an operational limitation.
5. The reflection coefficient:

$$R_i = [E_i/E_{in}]^{1/2} \tag{3}$$

   where E_{in} is the total incident energy entering i^{th} layer and assuming

$$E_{in} = E_o - \sum_{j=1}^{i-1} E_j \tag{4}$$

6. Acoustic Impedance

$$Z_i = Z_w \frac{1+R_n}{1-R_n} \tag{5}$$

   where Z_w is the impedance of sea water.

   The impedance calculations were made relative to water initially so that Hamilton's soil classification tables could be utilized directly. A typical table of impedance versus material type is shown in Table 1.
7. Impedance versus Time and Depth: Depending on the field reference cores, various algorithms are utilized to generate both impedance versus time and impedance versus depth. Figure 3 is a typical plot of the latter.

Impedance	Material
1550 - 2061	Water
2062 - 2573	Silty Clay
2574 - 3085	Silty Sand
3085 - 3594	Very Fine Sands
3595 - 4109	Medium Sands
4109 - 5133	Course Sands/Gravel
5134 - greater	Consolidated Material

Table 1. Typical table of impedance versus material type.

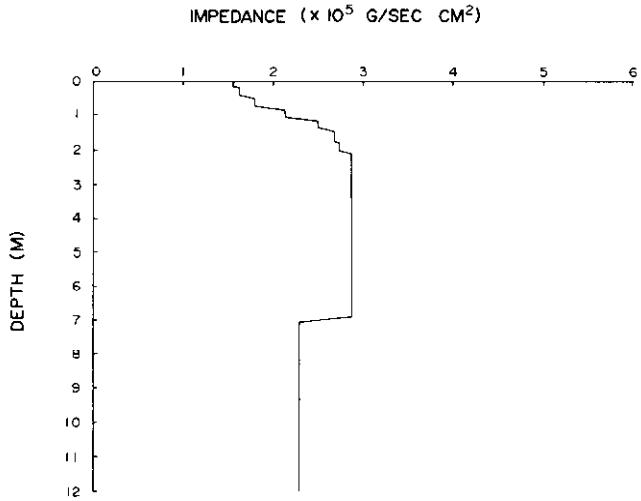

Fig. 3. Acoustic core - impedance versus depth.

The system generates these precision impedance plots and/or a graphic algorithm generates impedance cross sections versus travel time based solely on the centre frequency of the source. These impedance values are assigned colour codes. The typical colour codes are given in Table 2 and a cross section of data processed in colour is shown in Figure 4. The application of these procedures to various locations around the world in the last two years has delineated specific areas where immediate improvements can be made in reflection and absorption modelling. These are addressed in the next two sections.

Impedance	Colour Code
1500 - 1900	white white white
1900 - 2100	yellow yellow yellow
2100 - 2300	yellow yellow red
2300 - 2500	yellow red red
2500 - 2700	red red red
2700 - 2900	red red blue
2900 - 3100	red blue blue
3100 - 3300	blue blue blue
3300 - 3500	green green green
3500 - greater	purple

Table 2. Impedance versus colour codes.

Reflectivity Algorithm

The original algorithm used in the Acoustic Core System was a first approximation of the correct procedure for calculating the reflection coefficients. Equation (3) above gives the procedures. A second approximation, taking into account the primary internal reflections (see Fig. 5), takes the form of:

$$R_i^2 = E_i / [E_o \prod_{j=1}^{i-1} (1-R_j^2)^2] \tag{6}$$

where E_o = the total energy
E_i = the energy reflected from the i^{th} layer after correcting absorption loss and spherical spreading
R_i = the amplitude reflection coefficient from the i^{th} layer

Assuming that E_o is known, this formula improves results by about 5% over the simpler algorithm, depending on the number of reflectors. All reflected energies are corrected for absorption by a simple exponential model that approximates Hamilton's original data.

However, a major difficulty with both algorithms arises when attempting to estimate E_o. Hitherto, E_o has been estimated from the formula:

$$E_o = K \sum_{i=1}^{N} E_i \tag{7}$$

That is, the incident energy is the sum of the absorption-corrected reflected energies times a correction constant K. K represents the energy "lost" by reflection downward into the earth. N is the total number of layers. K has previously been determined empirically for each region of investigation. We have,

$$K = \frac{E_o}{\sum_{i=1}^{N} E_i} \tag{8}$$

Rearranging (6) and summing gives

$$\sum_{i=1}^{N} E_i = E_o \sum_{i=1}^{N} [R_i^2 \prod_{j=1}^{i-1} (1-R_j^2)^2] \tag{9}$$

Substituting (9) into (8), we obtain:

$$K = 1 / [\sum_{i=1}^{N} (R_i^2 \prod_{j=1}^{i-1} (1-R_j^2)^2)] \tag{10}$$

The K factor is therefore completely determined by the reflectivities of the stratified sub-bottom.

The approach used is to estimate K from raw seismic data, borehole data, or past experience in the region. This first estimate depends primarily on the number of layers present, since the variation in reflectivities is generally small for a given region of investigation.

Given the first K estimate, the reflectivity values are calculated; K is then recalculated by using (10). Convergence of this algorithm, illustrated in Figure 6, is not always consistent, particularly when the number of layers is greater than three.

If R_1 is known to a high degree of accuracy, by analysis of the sea-bottom multiples for example, another approach is possible. By rearranging (6) and taking any two successive reflected energies, we see:

$$\frac{E_i}{E_{i+1}} = \frac{R_i^2 \prod_{j=1}^{i-1} (1-R_j^2)^2}{R_{i+1}^2 \prod_{j=1}^{i} (1-R_j^2)^2} \tag{11}$$

The troublesome E_o is thus eliminated. The equation reduces to

$$\frac{E_i}{E_{i+1}} = \frac{R_i^2}{R_{i+1}^2 (1-R_i^2)^2} \tag{12}$$

Rearranging, we obtain a formula for R_{i+1}.

$$R_{i+1}^2 = \frac{E_{i+1} R_i^2}{E_i (1-R_i^2)^2} \tag{13}$$

Given R_1, we can therefore determine the succeeding reflectivities. All practical attempts to solve theoretical inverse problems involve the isolation of the uncertainty in one variable, and the use of outside information to estimate that variable. For example, if R_1 is not known accurately, one approach is to use an average

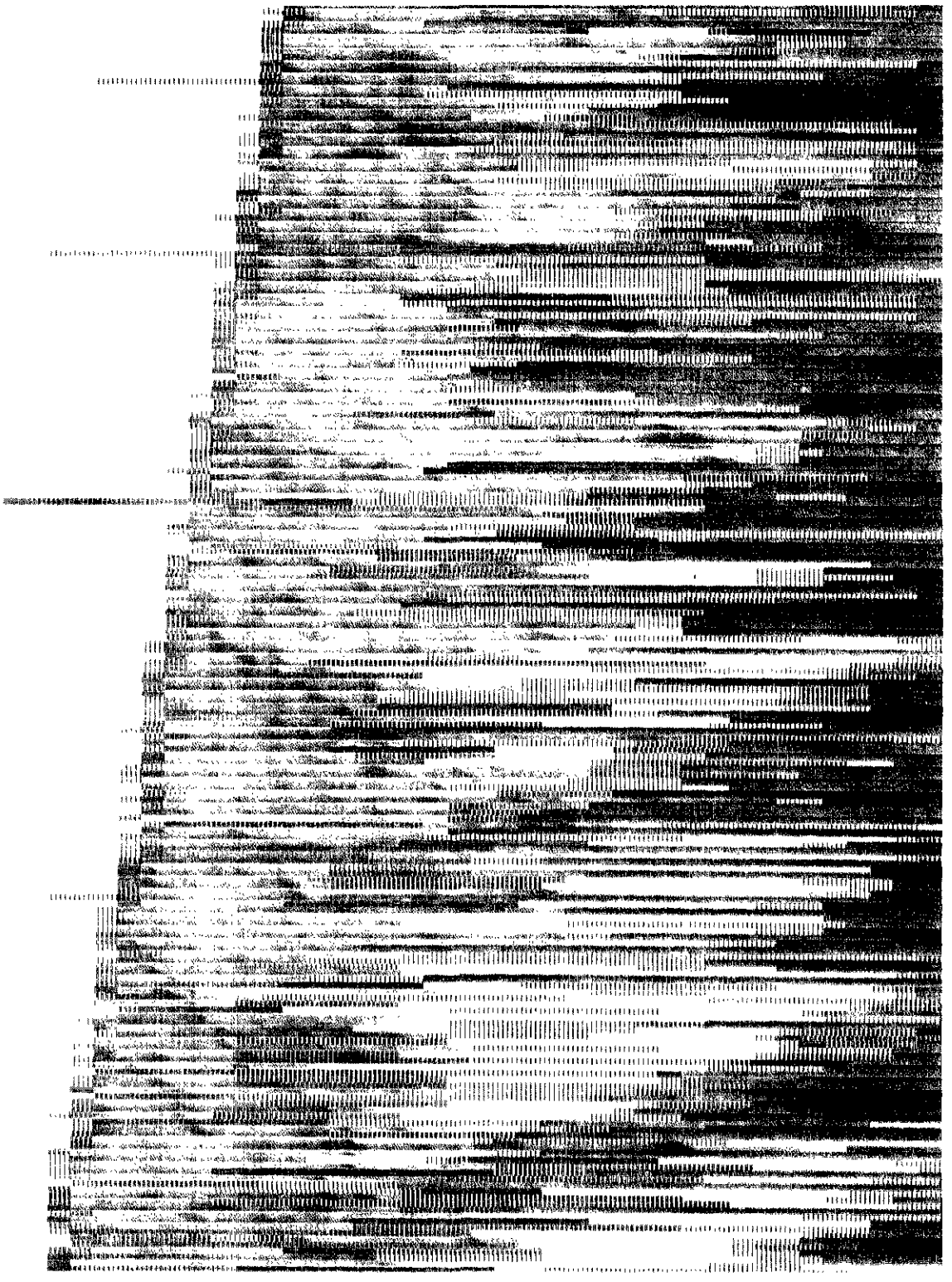

Fig. 4. Colour section.

reflectivity value for the region to estimate K, and then one can estimate R_I from the equation:

$$R_I^2 = \frac{E_I}{K \sum_{i=1}^{N} E_i} \qquad (14)$$

A comparison of processing techniques is presented in Table 3.

Absorption Model

The traditional approach to modelling absorption losses involves an exponential factor that is dependent on

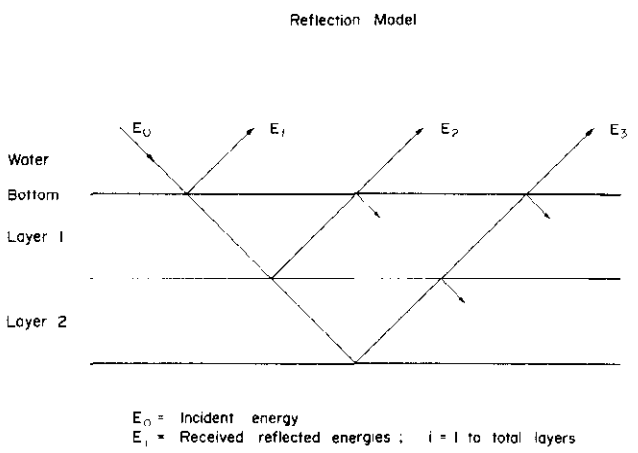

Fig. 5. Reflection model.

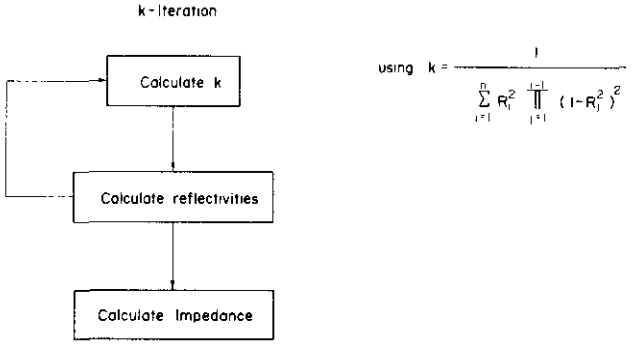

Fig. 6. K-iteration.

Layer	True R	Original Algorithm	K-Loop Algorithm	R_1 Known
1	0.200	0.230	0.204	0.200
2	0.300	0.340	0.307	0.300
3	0.200	0.220	0.201	0.195

Table 3. Comparison of reflectivity algorithms.

frequency, velocity, density, and an empirically derived constant. It is clear, however (see Fig. 7), that this exponential factor is only an approximation of the actual absorption found in marine sediments (Hamilton *et al.*, 1970). Although there has been some success in developing an empirical approach to this problem (Hamilton, 1972), a complete theoretical model of absorption losses in saturated sediments has not yet been developed. The complexities of transmission in viscoelastic solids with an infinite variety of grain size, shape and type, are well represented in the literature (Hamilton, 1971a). There is also the problem of compaction, which again is difficult to predict theoretically, but experimentally can be estimated (Hamilton, 1971b).

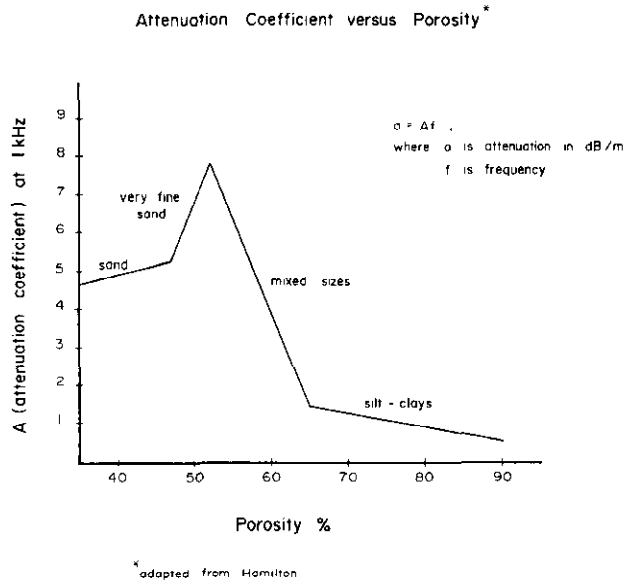

Fig. 7. Attenuation coefficient versus porosity.

Hamilton and Bachman's work demonstrates that the ordinary exponential absorption model is incomplete. The only alternative is to use empirical data collected by various researchers, in particular Hamilton and Bachman, 1982.

The importance of a correct absorption model is illustrated by the difficulties encountered when the first absorption model was used in a fluvial environment. Although the region was dominated by terriginous sediments, differences in deposition, salinity, and depth of the bottom apparently cause the system to underestimate absorption.

The absorption variation with porosity is complex, and there is considerable deviation from Hamilton's regression curves. Hamilton suggests that the curve (see Fig. 7) derives its shape from changes in the way sediment particles interact with each other at different porosities.

Though a general theory of absorption might be possible, in view of the availability of high-quality experimental data it seems prudent to attempt to define an empirical absorption model.

Hamilton reports that absorption varies as

$$a = kf^n \qquad (15)$$

where a = attenuation in db/m
f = frequency
k = attenuation coefficient

Hamilton suggests n = 1

The complete model, including variation with depth, would take the form of a two-dimensional matrix, assuming the supposedly independent variables, depth and porosity, are used. Density may be substituted for porosity, since there is a direct empirical relationship

between porosity and density. The matrix formula of this is:

$$E_I = A\,E_N \tag{16}$$

$$A = \begin{bmatrix} a(D_1, \phi_1) & a(D_1, \phi_2) & \ldots & a(D_1, \phi_n) \\ a(D_2, \phi_1) & a(D_2, \phi_2) & \ldots & a(D_2, \phi_n) \\ \cdot & \cdot & & \cdot \\ \cdot & \cdot & & \cdot \\ \cdot & \cdot & & \cdot \\ a(D_n, \phi_1) & a(D_n, \phi_2) & \ldots & a(D_n, \phi_n) \end{bmatrix} \tag{17}$$

where E_I = corrected energy array
A = matrix correction factors
E_N = uncorrected energy array

The difficulty with empirical models is that in unusual circumstances they produce incorrect results. Examples include:

1. Arctic sediments — it is uncertain whether arctic sediments coincide with Hamilton's data.
2. Gas Hydrates — the presence of gas in sediments causes large changes in impedance.
3. Permafrost — almost nothing is known about the effects or detection of permafrost on shallow records.
4. Extreme compaction — surficial sediments that have undergone compaction — for example, arctic sediments under ice — might have higher velocities and densities.
5. Bioturbation — in some areas of the world biologic effects, such as root-system and worm tracks, might have a significant impact in the top few metres.
6. Alternate depositional models — in regions whose principal depositional source is not terrigenous, alternate curves must be added.

Many of Hamilton's curves, such as impedance versus porosity, and porosity versus absorption, display such a good fit to the regression equations that an iterative approach to absorption corrections is attractive. The iteration algorithm is described in Figure 8.

Preliminary use of the absorption algorithm demonstrated the feasibility of the technique; however, computation time is increased roughly four times.

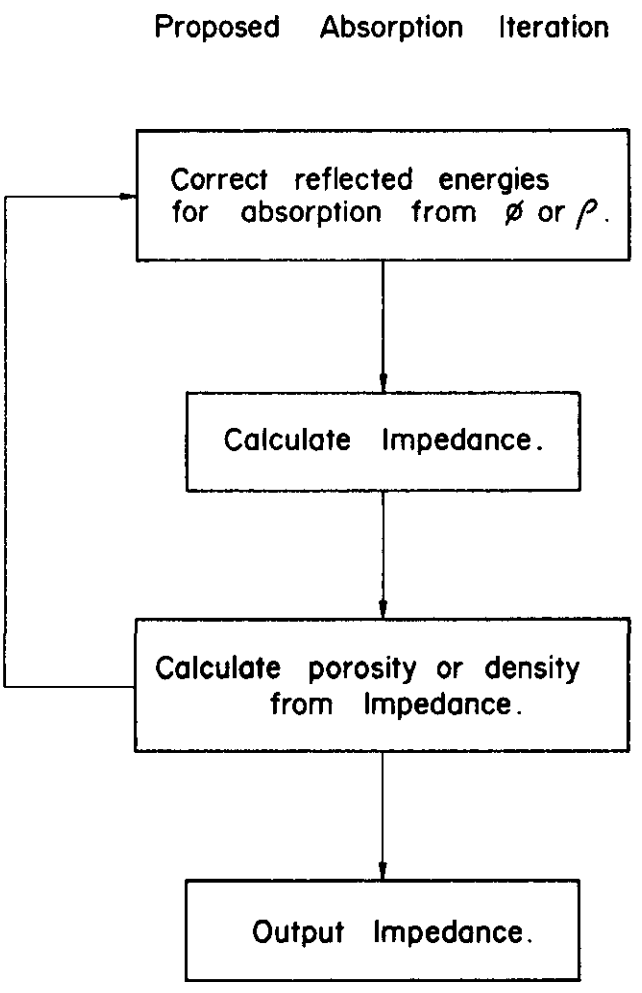

Fig. 8. Proposed absorption iteration.

CONCLUSIONS

Recent theoretical and practical investigations have shown that sub-bottom impedance modelling can be significantly improved in the following areas:

1. Reflectivity algorithms - An improved reflectivity algorithm has been shown to improve both processing time and results. One of the main features of this algorithm is its ability to accept empirical data.
2. Absorption Model - Since absorption corrections can be an order of magnitude greater than the other loss mechanisms such as spherical spreading, use of an empirically derived, flexible absorption model is essential for a comprehensive sub-bottom model. Data for an empirical study are readily available from the work of many researchers.

Other programming and algorithm improvements are at present being developed; they include multiple removal, and use of correlation techniques to compute reflection coefficients. It is interesting to note that when multiples are available, the initial coefficient can be calculated independently from these data, leading to further verification procedures.

REFERENCES

Bachman, R.T. 1985. Acoustic and physical property pelationships in marine sediments. Unpublished.

Biot, M.A. 1985. Theory of propagation of elastic waves in a fluid-saturated porous solid. II. Higher frequency range. Journal of Acoustical Society of America, v. 28, no. 2, p. 179-191.

Breslau, L.R. 1964. Sound Reflection from the Sea Floor and its Geological Significance. Ph.D. Thesis, Massachusetts Institute of Technology, June 1964.

Caulfield, D.D. and Faas, R. 1970. Determination of the bulk properties of saturated sediments through spectral analysis. AAPG-SEPM National Meeting, Calgary, Alberta, June 27.

Caulfield, D.D., Liron, A., Lewis, D.F.M. and Hunter, J.A. 1976. Preliminary test results of the banques through ice sub-bottom acoustic profiling system at Tuktoyuktuk, N.W.T. Geological Survey of Canada, Paper 76-1A.

_____ and Yim, Yung-Chang. 1982. Prediction of shallow sub-bottom sediment acoustic impedance estimating absorption and other losses. Canadian Society of Exploration Geophysicists Conference, Calgary, December 1983, v. 19, no. 1.

_____, Yim, Yung-Chang and McGee, T. 1983. Applications of the auto correlation factors for layer identification in shallow seismics. Canadian Society of Exploration Geophysicists Conference, Calgary.

_____, 1984. Shallow seismic derived acoustic core logs. Paper 4720, 16th Annual Offshore Technology Conference, Houston, Texas.

_____, McKenzie, K.J. and Stirbys, A.F. 1984. The use of processed high-resolution seismic data in geotechnical engineering. Offshore Technology Conference, OTC 4719.

Hamilton, E.L. 1970. Reflection coefficients and bottom losses at normal incidence computed from Pacific sediment properties. Geophysics, v. 35, p. 995-1004.

_____, Bucker, H.P., Keir, D.L. and Whitney J.A. 1970. Velocities of compressional and shear waves in marine sediments determined IN-SITU from a research submersible. J. Geophysical Res., v. 75, p. 4049.

_____, 1971a. Elastic properties of marine sediments. J. Geophysical Res., v. 76, p. 579-604.

_____, 1971b. Prediction of IN-SITU acoustic and elastic properties of marine sediments. Geophysics, v. 36, p. 266-284.

_____, 1972. Compressional-wave attenuation in marine sediments. Geophysics, v. 37, p. 620-646.

_____ and Bachman, R.T. 1982. Sound velocity and related properties of marine sediments. Journal of Acoustical Society of America, v. 72, p. 1891-1904.

Helstron, C.W. 1960. Statistical Theory of Signal Detection. Pergamon Press.